Analytical Methods

Accepted Manuscript

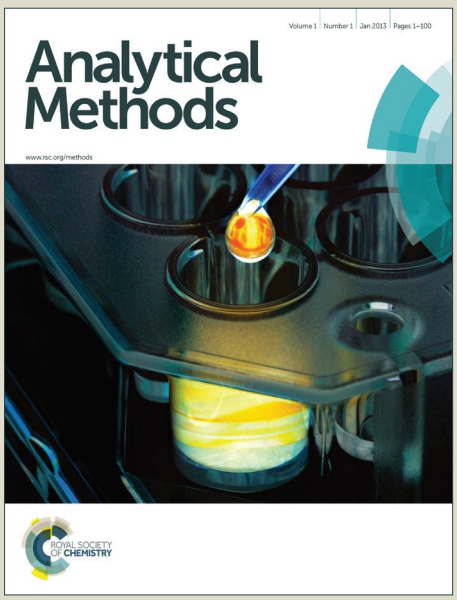

This is an *Accepted Manuscript*, which has been through the Royal Society of Chemistry peer review process and has been accepted for publication.

Accepted Manuscripts are published online shortly after acceptance, before technical editing, formatting and proof reading. Using this free service, authors can make their results available to the community, in citable form, before we publish the edited article. We will replace this *Accepted Manuscript* with the edited and formatted *Advance Article* as soon as it is available.

You can find more information about *Accepted Manuscripts* in the Information for Authors.

Please note that technical editing may introduce minor changes to the text and/or graphics, which may alter content. The journal's standard Terms & Conditions and the Ethical guidelines still apply. In no event shall the Royal Society of Chemistry be held responsible for any errors or omissions in this *Accepted Manuscript* or any consequences arising from the use of any information it contains.

ROYAL SOCIETY OF CHEMISTRY

www.rsc.org/methods

Chemical Identification of Cannabinoids in Street Marijuana Samples using Electrospray Ionization FT-ICR Mass Spectrometry

Iendel R. Nascimento[1], Helber B. Costa[1], Lindamara M. Souza[1], Letícia C. Soprani[1], Bianca B. Merlo[3], Wanderson Romão[1,2†]

[1] Laboratório de Petroleômica e Forense, Departamento de Química, Universidade Federal do Espírito Santo, Avenida Fernando Ferrai, 514, Goiabeiras, Vitória – ES, CEP: 29075-910.

[2] Instituto Federal do Espírito Santo, Av. Ministro Salgado Filho, Soteco, Vila Velha- ES, CEP: 29106-010.

[3] Laboratório de Química Legal, Superintendência de Polícia técnico-científica da Polícia Civil do Estado do Espírito Santo, Rua José Farias s/ n, Santa Lúcia, Vitória – ES, CEP: 29045-300.

Correspondent Authors

† W. R : wandersonromao@gmail.com / Phone: + + 55-27-3149-0833

Abstract

The C*annabis sativa L.* plant is a species rich in a variety of cannabinoid compounds and the Δ^9-tetrahydrocannabinol (Δ^9-THC) has been reported as a main psychotropic substance. In this study, electrospray ionization (ESI), coupled with Fourier transform ion cyclotron resonance mass spectrometry (FT-ICR MS), was used in order to perform a direct and fast analysis of street marijuana samples. ESI(-)-FT-ICR MS detected 21 cannabinoid species in deprotonated form, $[M - H]^-$. Other species were detected in regions of *m/z* 600–800 and 800–1000, corresponding to dimers and trimers of cannabinoids. In addition, the ESI(-) was better able to analyze the chemical profile of terpenophenolic species ($C_cH_hO_o$) than ESI(+). ESI(+)-FT-ICR MS detected the presence of adulterants such as cocaine, lidocaine, and nicotine, respectively. Finally, the sensibility of fast blue B colorimetric testing was also evaluated and the results were compared to the ESI(-)FT-ICR MS data.

Keywords: marijuana; Δ^9-THC; c*annabis;* FT-ICR MS*;* mass spectrometry

1. Introduction

Cannabis sativa L., a plant that originated in central Asia, has been cultivated as a source of fiber, fodder, oils, medicines, and intoxicants for thousands of years. It is also used worldwide as an illicit drug popularly known as marijuana. In Brazil, it is called "maconha," and it presents psychotropic substances such as Δ^9-tetrahydrocannabinol (Δ^9-THC) [1,2]. Its planting, cultivation, harvesting, exploitation, and consumption are prohibited.

Cannabis plants (*sativa, indica,* and *ruderalis*) are rich in a variety of cannabinoid compounds and are composed of more than 120 terpenophenolic species divided into nine subclasses: Δ^9-tetrahydrocannabinol; cannabidiol; cannabielsoin; cannabitriol; cannabichromene; cannabigerol; Δ^8-tetrahydrocanabinol; cannabinol/cannabinodiol and cannabicyclol (**Figure 1**) [1,2].

Δ^9-THC (6a, 10a-trans-6a, 7,8,10 a-tetrahydro-6,6,9-trimethyl-3-pentyl-6H-dibenzo [b, d] pyran -1-ol), the main psychoactive substance found in marijuana (**Figure 1a**), is present in the Δ^9-tetrahydrocannabinol class. Besides Δ^9-THC (M_w = 314 Da), there are eight cannabinoid species, distinguished by their side chains, which range from one to five carbons (R_2 =C_5H_{11}, C_4H_9, C_3H_7, and CH_3; **Figure 1a**). The main biogenic precursor of Δ^9-THC is the Δ^9-THCA-A (Δ^9-tetrahydrocannabinolic acid A, M_w = 358 Da). However, five other isomers of Δ^9-THC can exist in marijuana samples: cannabichromene (CBC) **(Figure 1e);** cannabidiol (CBD) (**Figure 1h);** Δ^8-*trans*-(6aR,10aR)-tetrahydrocannabinol (Δ^8-trans-THC) (**Figure 1f);** Δ^9-6aS,10aR-*cis*-tetrahydrocannabinol ((-)-*cis*-Δ^9-THC) (**Figure 1a);** and (±)-1aS,3aR,8bR,8cR-cannabicyclol (CBL) (**Figure 1i).** Among them, the CBD constitutes up to 40% of cannabis extracts and is devoid of the typical psychological effects of cannabis in humans. In generally, CBD have anxiolytic and/or antipsychotic actions [3], whereas the most of other isomers of Δ^9-THC exhibit non-biological activity [2].

Cannabigerol, that is a nonpsychotropic cannabinoid, (CBG, where R_1 = H, R_2 = C_5H_{11} and R_3 = H, M_w = 316 Da) was first identified in 1964 from its precursor, cannabigerolic acid (CBGA, where R_1 = COOH, R_2 = C_5H_{11} and R_3 = H M_w = 360 Da). The CBG shows sedative effects, antitumour activity against human cancer cells and has antibiotic properties [4]. This class has a side chain propyl group and a monomethyl ether derivative as a basic structure (**Figure 1f**). Cannabidiol (CBD, R_1 = H, R_2 = C_5H_{11} and R_3 = H, M_w = 314 Da; **Figure 1g**) was isolated in 1940, but its correct structure was elucidated in 1963 by Mechoulam and Shvo [8]. This class features seven other different cannabinoids with side chains ranging from C_1 to C_5. Among them, cannabidiolic acid (CBDA, R_1 = COOH, R_2 = C_5H_{11} and R_3 = H, M_w = 358 Da; **Figure 1g**), which

constitutes the most abundant cannabinoid found in fiber-type cannabis (used in the hemp industry), was isolated in 1955. There are also eight other different cannabinoid types of cannabinol and cannabinodiol classes. All are derived from the oxidation of Δ^9-THC and CBD, and their concentration depends on the age and storage conditions of the *Cannabis sativa* plant. [2-9]

Figure 1

Forensic laboratories analyze marijuana samples mainly by using colorimetric testing kits, which are often based on the fast blue B salt or Duquenois–Levine tests. These tests are based on the development of specific colors, such as purple-red or blue, when Δ^9-THC, CBN, and CBD cannabinoids are present, producing an extract soluble in the organic phase. However, in some cases, it can lead to false positive results in the presence of plants such as *Jacaranda decurrens cham*. and *Paullinia cupana Kunth* [10]. Therefore, it is important to explore and elucidate the chemical composition of marijuana samples.

Ultra-high resolution and accuracy mass spectrometry, such as Fourier transform ion cyclotron resonance mass spectrometry (FT-ICR MS), is a powerful tool that enables the identification of complex organic mixtures without prior extraction or separation steps. FT-ICR MS is applied in all of the "omics" sciences (i.e., metabolomics, proteomics, and petroleomics), as it enables molecular-level analysis of complex mixtures. Accurate mass measurements define a unique elemental composition ($C_cH_hN_nO_oS_s$) from singly charged ions, such as $[M + H]^+$, $[M + Na]^+$, $[M + K]^+$, $[M - H]^-$, and $[M + Cl]^-$, where M corresponds to a neutral molecule [11-15]. Within this context, electrospray ionization (ESI), coupled with FT-ICR MS (allied to chemometric tools), has been used in the direct and fast analysis of street marijuana samples, classifying them by presence of cannabinoids and adulterants. In addition, the sensibility of the fast blue B colorimetric test was evaluated to detect the presence of cannabinoids in different parts of the *Cannabis sativa* plant (leaves, seeds (achene)* or fruits of cannabis, flowers, and stem), and the data were compared with the ESI-FT-ICR measurements.

2. Experimental Procedure

2.1 Samples and reagents

* The seed is actually a fruit, or technically, an achene. It contains a single seed with a hard shell.

Forty-three marijuana samples seized in different regions of the state (capital, north, south, and northwest), the *Cannabis sativa* plant (seeds, leaves, and flower), and hashish samples (concentrated Δ^9-THC) were supplied by the Civil Police of Espírito Santo, Vitória, Brazil.

Acetonitrile (ACN), methanol, dichloromethane (CH_2Cl_2), and petroleum ether (analytical grades with purity >99.5%) were supplied by Vetec Química Fina Ltda, Brazil, and used for the extraction step. Fast Blue B salt (containing di-*o*-anisidine tetrazolium chloride), ammonium hydroxide (NH_4OH), sodium trifluoroacetate (NaTFA), arginine, and formic acid (HCOOH) were purchased from Sigma–Aldrich Chemicals USA and used for colorimetric testing and ESI(±)-FT-ICR MS measurements. All reagents were used as received.

2.2 Solution preparation

Three different solutions (ACN, methanol, and a methanol:DCM [50:50 v/v %] mixture) were evaluated for an easy and fast solid–liquid extraction of Δ^9-THC and other cannabinoids from typical marijuana samples. Briefly, three marijuana samples were weighted (each sample containing 2 mg) into three microtubes and mixed separately with 1 mL of ACN, methanol, and methanol:DCM. After each solution was stirred for 5 min (using a Vortex mixer) and centrifuged, the remaining solution was acidified or basified and analyzed by ESI(±)FT-ICR MS. The efficiency of extraction was evaluated from the MS data, and the optimized method was used for the other marijuana (42), hashish (2), flower (2), leaf (2), and seed (3) samples.

2.3 ESI(±)-FT-ICR MS

Briefly, marijuana (2 mg mL^{-1}), hashish, seed, flower, and leaf extracts (15 mg mL^{-1}) were prepared in acetonitrile containing 1% m/v of NH_4OH (28-30 % in volume) for ESI in negative mode, ESI(-), and 1% m/v of formic acid for ESI in positive mode, ESI(+). The supernatant solution was directly infused at a flow rate of 5 μL min^{-1} into the ESI source. The mass spectrometer (model 9.4 T Solarix; Bruker Daltonics, Bremen, Germany) was set to operate over a mass range of 200–2000 *m/z*. The ESI source conditions were as follows: nebulizer gas pressure of 3 bar, capillary voltage of 2.5-4.1 kV, and transfer capillary temperature of 250°C. The ions were accumulated in the hexapolar collision cell in 0.02 s, followed by transport to the analyzer cell (ICR) through the multipole ion guide system (another hexapole). The time-of-flight in the hexapole was 0.9 ms. Each spectrum was acquired by accumulating 32 scans of time-domain transient signals in 4 mega-point time-domain data sets. All mass spectra were externally calibrated using NaTFA (*m/z* 200–2000). A resolving power, $m/\Delta m_{50\%} \cong 530\,000$, in which $\Delta m_{50\%}$ is the full peak width at a half-maximum peak height of *m/z* ≅ 400 and a mass accuracy of < 3

ppm, provided the unambiguous molecular formula assignments for singly charged molecular ions. Mass accuracy is determined from mass error, defined as Error = (($m/z_{measured}$ – $m/z_{theoretical}$)/$m/z_{theoretical}$) x 10^6. The mass spectra were acquired and processed using Data Analysis software (Bruker Daltonics). The MS data were processed, and the elemental compositions of the compounds were determined by measuring the *m/z* values. The aromaticity of each molecule was deduced directly from its DBE (double bond equivalent) value as follows [11,12]:

$$DBE = c - h/2 + n/2 + 1 \quad (\textbf{Equation 1})$$

where c, h, and n are the numbers of carbon, hydrogen, and nitrogen atoms, respectively, in the molecular formula. [16]

2.4 ESI(-)FT-ICR MS/MS

The tandem mass spectrometry (MS^2) experiments were performed on a quadrupole analyzer coupled to the FT-ICR mass spectrometer, Q-FT-ICR MS. The ESI(-)-MS/MS spectra were acquired using: **i)** infusion flow rate of 5 μL min^{-1}; **ii)** capillary voltage of 3.0 kV; **iii)** nebulizing temperature of 250°C; **iv)** argon as collision gas; **v)** ion accumulation time of 1 s; **vi)** isolation window of 1.0 (*m/z* units); **vii)** and 25–45% of the collision energy. The spectra were acquired by accumulating 32 time-domain transient scans and processed using Data Analysis software.

2.5 Colorimetric test

Ten marijuana samples were selected and submitted to colorimetric test using fast blue B salt. Briefly, 2 mg of each sample were weighted and dissolved in petroleum ether. From the organic extract (≅ 2 mg mL^{-1}), an aliquot of 100 μL was spotted on the surface of filter paper. After the solvent evaporated, fast blue B salt (20 mg) and a NaOH solution (100 μL) were added to each spot. The colorimetric test was also performed on the hashish, flower, seed, and leaf samples. The emergence of a red-purple color is indicative of the presence of cannabinoids in marijuana samples.

The limit of detection (LOD) for the colorimetric test was evaluated in duplicate using marijuana solutions ranging from 20 to 0.06 mg mL^{-1} prepared from a stock solution (20 mg mL^{-1} concentration).

2.6 Chemometric analysis

ESI(+)FT-ICR MS data were processed to generate a final data matrix containing 3801 variables (*m/z* values detected in the 200–1200) for the 43 samples analyzed. For the classification of the marijuana samples, a principal component analysis (PCA) was performed on the MS data using PLS-Toolbox 4.02 for Matlab v. 7.0.1 software.

3. Results

3.1 ESI(+)-FT-ICR MS

Figures 2a–c show ESI(+)-FT-ICR mass spectra for a typical organic extract of marijuana obtained using **(a)** ACN, **(b)** methanol/DCM (1/1% v/v), and **(c)** methanol solvents. Generally, a higher number of signals is detected in the 300–800 *m/z* regions for marijuana extract obtained from ACN solvent (**Figure 2a**), in which the main active ingredients, such as Δ^9-THC and CBN-C_5, are detected in protonated form, $[\Delta^9\text{-THC} + H]^+$ and $[CBN + H]^+$, corresponding to ions of *m/z* 315.2321 and 311.2008. The accurate *m/z* values (315.2321 and 311.2008) are also in agreement with the calculated *m/z* values (315.2319 and 311.2006), detected with mass deviations lower than 1 ppm. The DBEs of 7 and 9 for the Δ^9-THC and CBN-C_5 molecules indicate the presence of one aromatic ring (DBE = 4), a furan ring (DBE = 1), and cyclohexene (DBE = 2 for Δ^9-THC) and 1,3-cyclohexa-diene (DBE = 3 for CBN-C_5), as illustrated in **Figure 1**. Accurate mass measurement can be used, therefore, for a more accurate identification of the chemical profile of cannabinoid species present in illicit drugs such as marijuana samples. ACN was the choice of work solvent for cannabinoid extraction from marijuana samples, hashish, and parts of the *Cannabis* plant.

Figure 2

Figures 3a–d show the ESI(+)-FT-ICR mass spectra of four marijuana samples seized by the Brazilian Civil Police: I (**3a**), II (**3b**), III (**3c**), and IV (**3d**). Typical chemical fingerprints of cannabinoid molecules can be seen in samples I (**Figure 3a**) and IV (**Figure 3d**), detected in three distinct *m/z* regions: 200–400, 600–800, and 800–1000. They correspond to monomers, dimers, and trimers of cannabinoids, identified as $[M + H]^+$, $[2M + H]^+$ or $[M + N + H]^+$, and $[2M + N + H]^+$, where M and N correspond to specific cannabinoid molecules, as illustrated in **Figure 1**.

Among the 43 marijuana samples analyzed, Δ^9-THC was confirmed by ESI(+)-FT-ICR MS in 27 samples. The presence of adulterants such as cocaine (ion [M + H] of *m/z* 304.1551, **Figure 3c**, detected in 28 samples), lidocaine (ion [M + H] of *m/z* 235.1806,

Figure 3a, detected in 14 samples), and ions of *m/z* 491.3276, 819.5321, and 1147.7387, (**Figures 3b and c,** present in 25 samples) suppress the chemical ionization of cannabinoid molecules that present lower basicity (lower pKa values), which can provide false negative results for the Δ^9-THC molecule. Note that this approach does not lead to quantitative results, due to inherent, large differences in ionization efficiencies among the heteroatom species, but permits a proper comparison and qualitative evaluations of results.

Figure 3

The ions of *m/z* 491, 819, and 1147 correspond to a new adulterant not reported in the literature from FT-ICR MS data. ESI(+)-FT-ICR MS provides molecular weight (M_w), DBE, and accuracy of mass values for the ions of *m/z* 491, 819, and 1147 that correspond to $C_{31}H_{42}N_2O_3$ (DBE = 5 and error = -1.6 ppm), $C_{52}H_{70}N_2O_6$ (DBE = 19 and error = -2.4 ppm), and $C_{73}H_{98}N_2O_9$ (DBE = 26 and error = -3.9 ppm), respectively, as shown in **Figures 4a–c**.

To confirm the structures and the connectivity of this new adulterant, the ESI(+)-MS/MS spectra were acquired for the ions $[C_{31}H_{42}N_2O_3 + H]^+$, $[C_{52}H_{70}N_2O_6 + H]^+$, and $[C_{73}H_{98}N_2O_9 + H]^+$ of *m/z* 491, 819, and 1147 (**Figures 4a–c**), respectively. This approach identified the characteristic loss and should confirmed the presence of the nicotine molecule (M = $C_{10}H_{14}N_2$ and DBE = 5) as an proposed adulterant, chemically attached to the OTHC (10-oxo-delta-6a(10a)-tetrahydrocannabinol) molecule (N = $C_{21}H_{28}O_3$ and DBE = 7; **Table 1**), derived from the Δ^9-THC class (**Figure 1a**).

Initially, as shown in **Figure 4a**, the CID experiment of ion $[C_{31}H_{42}N_2O_3 – H]^-$ of *m/z* 491 produced fragments with *m/z* 329, and 311, 287, and 271, in which the 491→329 and 329→311 transitions corresponded to the neutral losses of 162 Da (nicotine) and 18 Da (H_2O), respectively. The series of signals observed with *m/z* lower than 329 (311, 287, and 271) are attributed to the OTHC fragmentation. In addition, the ESI(+)MS/MS of the $[C_{52}H_{70}N_2O_6 + H]^+$ ion of *m/z* 819 (**Figure 4b**), produced main fragments of *m/z* 491 and 329 via neutral losses of 328 Da and 162 Da, corresponding to OTHC and nicotine molecules, respectively. Therefore, the ion $[C_{52}H_{70}N_2O_6 + H]^+$ of *m/z* 819 correspond to a dimer of OTHC linked to a nicotine molecule, also expressed as $[M + 2N + H]^+$, where M = $C_{10}H_{14}N_2$ and N = $C_{21}H_{28}O_3$. Finally, for the ESI(+)MS/MS spectrum of ion $[C_{73}H_{98}N_2O_9 + H]^+$ of *m/z* 1147, a similar fragmentation pattern is observed, confirming the presence of a trimer of OTHC plus one nicotine molecule (see **Figure 4c**, where two neutral losses of 328 Da [1147 → 819 and 819 → 491] and one of 162 Da [491→329] are identified).

Figure 4

3.2 ESI(-)-FT-ICR MS

It is well know that the presence of adulterants such as lidocaine, cocaine, and nicotine in street marijuana samples can suppress chemical ionization, mainly in positive ion mode, ESI(+); therefore, ESI(-)-FT-ICR mass spectra was acquired, as it is better able to analyze the chemical profile of terpenophenolic species that present a formula of $C_cH_hO_o$.

Figures 5a–d show the ESI(-)-FT-ICR mass spectra of the leaf **(5a)**, seed **(5b)**, hashish **(5c)**, and marijuana **(5d)** samples. Note that a higher number of cannabinoid species were detected in the hashish and marijuana samples. The ion of *m/z* 357.2070 is the more abundant species in the leaf, seed, and marijuana samples, corresponding to Δ^9-THCA-A. The ESI(-)-MS/MS experiments confirmed the structure and connectivity of this molecule (**Figure 6f**), where the ion $[C_{22}H_{30}O_4 - H]^-$ released H_2O (18Da) and CO_2 (44 Da) as neutral losses, producing fragments of *m/z* 313 (Δ^9-THC) and 245 [17]. Δ^9-THCA-A can undergo decarboxylation during storage and fermentation, and promptly during heating or smoking, converting to Δ^9-THC [18-22].

The magnification in the *m/z* region 300–400 identifies the main cannabinoids detected in deprotonated form: ion $[M - H]^-$ of *m/z* 309, 313, 327, 345, 353, 357, 389, and 399. Similar to ESI(+), dimers were also observed in ESI(-)-FT-ICR MS: ions $[M + N - H]^-$ of *m/z* 637, 653, 673, 681, 685, and 717, where M and N correspond to different cannabinoids. **Table 1** shows the formula, DBE, and measured and theoretical mass values of the cannabinoids identified from marijuana extracts analyzed by ESI(-)-FT-ICR MS.

Twenty-one cannabinoids were detected by ESI(-)FTMS (**Table 1**). A unique chemical structure is proposed for ions of *m/z* 295, 303, 307, 327, 331, 353, 361, 371,373, 387, 389, and 399. Other ions, such as *m/z* 257, 281, 285, 301, 309, 313, 329, 343, 345, and 357 [23-25] present constitutional isomers that can reach a maximum of six different structures, as in the case of the ion of *m/z* 313 (Δ^9-trans-THC, CBD, Δ^8-trans-THC, *cis*–Δ^9-trans-THC-C_5, CBL-C_5, and CBC-C_5). This context relates to chemical complexity of this type of plant extract, thus justifying the importance of the use of the FT-ICR MS technique.

The detected ions, shown in **Table 1**, can be better analyzed when grouped according to their respective chemical formulas. Ions of *m/z* 361, 367, 369, 371, 373, and 399, for instance, correspond to the O_5 class, with a $C_cH_hO_5$ formula where c = 21–24 and h = 24–32, and 7–11 DBE. In addition, ions of *m/z* 361, 371, and 373 correspond to 6a,7,10a-trihydroxy-Δ^9-tetrahydrocannabinol, Δ^9-THCA-A-8-one, and 11-hydroxy-Δ^9-THCA-A, respectively. The

ion of *m/z* 399 corresponds to a new chemical species not reported in the literature, which is derived from Δ^9-THCA. Ions of *m/z* 375, 377, 385, 387, and 389 correspond to the O_6 class, with a $C_cH_hO_6$ formula where c = 21–2 and h = 28–30, and 7–10 DBE. Finally, the ions of *m/z* 387 and 389 correspond to Δ^9-THCA-A-COOH and 8β,11-bis-hydroxy-Δ^9-THCA, respectively [17]. All chemical structures are shown in **Table 1S** (**supplementary material**).

Figure 5

Table 1

Figures 6a–h show ESI(-)-MS/MS for ions of *m/z* **(6a)** 309; **(6b)** 313; **(6c)** 327; **(6d)** 345; **(6e)** 353; **(6f)** 357; **(6g)** 389; and **(6h)** 399. The CID experiments for the ions of *m/z* 327, 345, 353, and 389 (**6c, d, e, and g,** respectively) present a similar fragmentation profile, in which, in all cases, a fragment of *m/z* 309 is produced. These structures should therefore present the CBN-C_5 compound in its basic core. On the other hand, the CID experiments for the ions of *m/z* 353 and 399 are similar to that of *m/z* 357 (ion [Δ^9-THCA - H]$^-$, **6f**), where the COOH group is identified by the neutral loss of 44 Da (CO2) via 353$\rightarrow$309 and 399$\rightarrow$355 transitions (**Figures 6e, h**).

Figure 6

Figure 7 shows the ESI(-)MS/MS for ions of *m/z* **(7a)** 637, **(7b)** 639, **(7c)** 641, **(7d)** 653, **(7e)** 673, **(7f)** 681, **(7g)** 685, and **(7h)** 718. A neutral loss of 328 Da corresponding to the CBC-C_5 molecule can be seen for ions of *m/z* 637 **(7a)**, 653 **(7d)**, 673 **(7e)**, 681 **(7f)**, 685 **(7g)**, and 718 **(7h)**, producing fragments of 309, 325, 345, 353, 357, and 389 *m/z*, respectively. A neutral loss of 314 Da (Δ^9-THC) can be seen for the ion of *m/z* 641 (**7c**), producing a fragment of *m/z* 327. These results confirm the structure and connectivity of the cannabinoids detected as dimers. There are two hypotheses that can explain the presence of dimers and trimers during the ionization process using ESI(±). The first is based on the natural presence of these molecules in the chemical composition of the c*annabis sativa L.* plant. For example, CBD in basic medium in the presence of oxygen undergoes an oxidation reaction, forming dimeric hydroxyquinones [8].

Another explanation is based on the cluster formation during the electrospray ionization. Campo et al., in 2009 [26], used FT-ICR MS to analyze a mixture of naphthenic acids (NA), which like cannabinoids, also form multimers. They attributed the natural

dimerization tendency of NA to the physicochemical mechanism of signal acquiring of FT-ICR MS. The dependence of signal intensities on the accumulation time within the hexapole ion trap suggests a non-covalent interaction as the primary cause of aggregation.

Figure 7

3.3 Colorimetric test

The colorimetric test using fast blue B test is the most common color reaction for visual detection of cannabinoid molecules in *Cannabis sativa L*. **Figure 8** shows the colorimetric tests of ten typical marijuana samples, hashish samples, and parts of the *Cannabis sativa L*. plant (flower, stem, leaves, and seeds). Note that positive results were observed in most cases (marijuana, hashish, flower, and stem), whereas negative results only occurred in the leaf and seed samples. These results are in good agreement with the ESI(-)-FT-ICR MS data that shows a lower cannabinoid concentration in the leaf and seed samples (**Figures 5a,b**).

Figure 8

The sensibility of the colorimetric test was also evaluated when the marijuana concentration was changed from 20 to 0.06 mg mL^{-1} (**Figure 9**). The visual detection of cannabinoids was reached at a minimum concentration (LOD) of 0.12 mg mL^{-1}.

Figure 9

3.4 Chemometric treatment

The ESI(+)-FT-ICR MS data were subjected to chemometric treatment via PCA (**Figure 10a,b**). PCA was used to evaluate statistically the performance of ESI(+)FTMS spectra in the classification of marijuana samples according to cannabinoids and adulterant concentrations. **Figures 10a** and **b** show PC1 *x* PC2 scores and loading plots, where the first two PCs account for about 41% of total variance. In the PC1 *x* PC2 scores plot, a separation into three large groups can be seen, corresponding to groups A (PC2 > 0), B (PC2 < 0), and C (PC2 ≅ 0), according to the PC2 region (**Figure 10a**). This separation is due mainly to the 304, 315, 491, 819, and 820 variables, where they have a significant influence for PC2 loading, as shown in **Figure 3b**. The first large group (group A) consists of marijuana samples with higher Δ^9-THC concentrations and the presence of cocaine; group B consists of

samples adulterated with nicotine; and group C consists of typical, non-adulterated marijuana samples.

Figure 10

4. Conclusion

Ultra-high resolution and accuracy mass spectrometry, such as Fourier transform ion cyclotron resonance mass spectrometry (FT-ICR MS), is a powerful tool for identifying terpenophenolic species in the C*annabis sativa L.* plant. Approximately 21 cannabinoid compounds were detected; among them, Δ^9-tetrahydrocannabinol (Δ^9-THC) was identified in both ionization modes ESI(±): *m/z* 313.2172 ($[M - H]^-$) and *m/z* 315.2321 ($[M - H]^-$).

Forty-three marijuana samples were analyzed in both ionization modes. The ESI(+)-FT-ICR MS data revealed cocaine (ion $[M + H]^+$ of *m/z* 304.1551), lidocaine (ion $[M + H]^+$ of *m/z* 235.1806), and nicotine (ions $[M + N]^+$, $[M + 2N]^+$, and $[M + 3N]^+$ of *m/z* 491.3276, 819.5321 and 1147.7387, respectively, where M = nicotine and N = OTHC cannabinoid) in most samples. Their structures and connectivity were confirmed by ESI(+)-MS/MS experiments. ESI(-)-FT-ICR MS detected 21 cannabinoids species in deprotonated form, $[M - H]^-$: ions of *m/z* 257, 281, 285, 295, 301, 303, 307, 309, 313, 327, 329, 331, 343, 345, 353, 357, 361, 371,373, 387, 389, and 399. Other species were detected in the 600–800 and 800–1000 *m/z* regions, corresponding to dimers and trimers of cannabinoids. In addition, the ESI(-) was better able than ESI(+) to analyze the chemical profiles of terpenophenolic species ($C_cH_hO_o$).

The FT-ICR MS data were subjected to chemometric treatment via PCA, in which a separation into three large groups was observed: group A contained higher Δ^9-THC concentrations and cocaine; group B contained samples adulterated with nicotine; and group C contained typical, non-adulterated marijuana samples.

The sensibility of the fast blue B colorimetric test was also evaluated to detect the presence of cannabinoids in different parts of the *Cannabis sativa* plant (leaves, seeds, flowers, and stem). Positive results were observed for most cases; negative results occurred only in the leaf and seed samples. The sensibility of this test was also evaluated when the marijuana concentration was changed from 20 to 0.06 mg mL^{-1}, where the visual detection of a red-purple color was reached at a minimum concentration (LOD) of 0.12 mg mL^{-1}.

5. Acknowledgments

The authors wish to thank the Civil Police for providing the marijuana samples and FAPES, CNPq, and CAPES for their financial support.

6. References

[1] M. A. Elsohly and D. Slade, *Life Sci*., 2005, **78**, 539.

[2] M. A. Elsohly, *Humana Press Inc. Totowa*, New Jersey, 2007.

[3] A.W. Zuardi, J.A.S. Crippa, J.E.C. Hallak, F.A. Moreira and F.S. Guimarães, *Braz J Med Biol Res,* 2006, **39**, 421.

[4] Franjo Grotenhermen, *Clin Pharmacokinet*, 2003, **42**, 327.

[5] Y. Shoyama, I. Yamauchi and V. Nishioka, *Chem. Pharm. Bull.*, 1970, **18**, 1327.

[6] R. Adams, M. Hunt and J. Clark, *J. Am. Chem. Soc.*, 1940, **196**, 199.

[7] R. Adams, B. Baker and R. Wearn, *J. Am. Chem. Soc.,* 1940, **8**, 2204.

[8] R. Mechoulam and L. Hanus, *Chem. Phys. Lipids*, 2002, **121**, 35.

[9] R. Mechoulam and Y. Shvo, *Tetrahedron*, 1963, **19**, 2073;

[10] D.C. Bordin, M. Messias, R. Lanaro, S.O. Cazenave and J. L. Costa, *Quim. Nova*, 2012, **35**, 2040;

[11] G. P. Dalmaschio, M. M. Malacarne, V. M. D. L de Almeida, T.M.C Pereira, A. O. Gomes, E. V. R. Castro, S. J. Greco, B. G. Vaz and W. Romão, *Fuel*, 2014, **115**,190;

[12] T. M. C. Pereira, G. Vanini, E. C. S. Oliveira, F. M. R. Cardoso, F. P. Fleming, A. C. Neto, V. L. Junior, E. V. R de Castro, B. G. Vaz and W. Romão, *Fuel,* 2014, **118,** 348.

[13] W. Romão, B. D. Sabino, M. I. S. Bueno, B. G. Vaz, A. C. Júnior, A. O. E. V. R. de Castro, R. A. Lordeiro, C. C. Nascentes, M. N. Eberlin and R. Augusti, *J. Foren. Sci.*, 2012, **57**, 1307.

[14] W. Romão, P. M. Lalli, M. F. Franco, G. Sanvido, N. V Schwab, R. Lanaro, J. L. Costa, B. D. Sabino, M. I. M. S. G. F. Sa, R. J. Daroda, V. Souza and M. N. Eberlin, *Anal. Bioanal. Chem.,* 2011, **400**, 3053.

[15] R. S. Ortiz, K. C. Mariotti, M. H. Holzschuh, W. Romão, R. Limberger and P. Mayorga, *Foren. Sci. Int.*, 2013, **229**, 13.

[16] C.A. Destefani, L. C. Motta, G. Vanini, L. M. Souza, J. F. A. Filho, C. J. Macrino, E. M. Silva, S. J. Greco, D. C. Endringer and W. Romão, *Microchem. J.*, 2014, 116, 216.

[17] J. Jung, M.R. Meyer, H.H. Maurer, C. Neusuß, W. Weinmanna and V. Auwartera, *J. Mass. Spectrom.,* 2009*,* **44***,* 1423.

[18] F.E. Dussy, C. Hamberg, M. Luginbül, T. Schwerzmann and T. Briellman, *Foren. Sci. Int.*, 2005, **3**, 149.

[19] T. Yamauchi, Y. Shoyama, H. Aramaki, T. Azuma and I. Nishioka, *Chem. Pharm. Bull.*, 1967, **15**, 1075.

[20] Y. Shoyama, I. Yamauchi and V. Nishioka, *Chem. Pharm. Bull.*, 1970, 18, 1327.

[21] G. S. Lewis and C. E. Turner, *J. Pharm. Sci.*, 1978, **67**, 876.

[22] R. K. Razdan, A. J. Puttick, B. A. Zitko and G. R. Handrick, *Experientia*, 1972, **28**, 121.

[23] M. Novotny, F. Merli, D. Wiesler, M. fenel and T. Saeed, *J. Chromatog.*, 1982, **238**, 141.

[24] R. Brenneisen, *Chemistry and analysis of phytocannabinoids and other cannabis constituents,* M. A. Elsohly ed., Totowa, New jersey, EUA, 2007.

[25] M.A. Elsohly and D. Slade, *Life Sci.*, 2005, **78**, 539.

[26] R. Da Campo, M.P. Barrow, A.G. Shepherd, M. Salisbury and P.J. Derrick, *Energy Fuels*, 2009, **23**, 5544.

Figure and Table Captions

Figure 1. Chemical structures of nine cannabinoid classes: **(a)** Δ^9-tetrahydrocannabinol; **(b)** cannabidiol; **(c)** cannabielsoin; **(d)** cannabitriol; **(e)** cannabichromene; **(f)** cannabigerol; **(g)** Δ^8-tetrahydrocanabinol; **(h)** cannabinol/cannabinodiol and **(i)** cannabicyclol.

Figure 2. ESI(+)FT-ICR mass spectra of marijuana extracts obtained from **(a)** ACN, **(b)** methanol/DCM (1/1% v/v), and **(c)** methanol.

Figure 3. ESI(+)-FT-ICR mass spectra of four marijuana samples: **(a)** I, **(b)** II, **(c)** III, and **(d)** IV. A typical chemical fingerprint is observed in three distinct *m/z* regions: 200–400, 600–800, and 800–1000. The presence of adulterants such as cocaine ([M + H]: *m/z* 304), lidocaine ([M + H]: *m/z* 235) and ions of *m/z* 491, 819, and 1147, however, can suppress the ionization chemical of cannabinoids.

Figure 4. ESI(+)-FT-ICR MS/MS for ions of *m/z* **(a)** 491, **(b)** 819, and **(c)** 1147.

Figure 5. ESI(-)-FT-ICR mass spectra of **(a)** leaf, **(b)** seed, **(c)** hashish, and **(d)** marijuana samples. The magnification in the region of *m/z* 300–400 identifies the main cannabinoids detected in deprotonated form: ions $[M - H]^-$ of *m/z* 309, 313, 327, 345, 353, 357, 389, and 399. Similar to ESI(+), dimers are also observed in the region of *m/z* 650 for ESI(-).

Figure 6. ESI(-)-MS/MS for ions of *m/z* **(a)** 309, **(b)** 313, **(c)** 327, **(d)** 345, **(e)** 353, **(f)** 357, **(g)** 389, and **(h)** 399.

Figure 7. ESI(-)-MS/MS for ions of *m/z* **(a)** 637, **(b)** 639, **(c)** 641, **(d)** 653, **(e)** 673, **(f)** 681, **(g)** 685, and **(h)** 718.

Figure 8. Colorimetric tests of ten typical marijuana samples and hashish, flower, stem, macerated leaf, seed, and blank samples using a basic fast blue B salt solution.

Figure 9. Colorimetric test as a function of marijuana concentration. The red-purple color is indicative of the presence of cannabinoids in marijuana samples, providing positive results from 20 mg mL^{-1} to 0.12 mg mL^{-1}.

Figure 10. (a) PCA scores and **(b)** loadings plots for ESI(+)-FT-ICR MS data. **Group A** includes marijuana samples with higher Δ^9-THC concentrations and group **B** includes samples adulterated with nicotine.

Table 1. Formula, DBE, and measured and theoretical mass values of the cannabinoids identified from marijuana extracts analyzed by ESI(-)-FT-ICR MS.

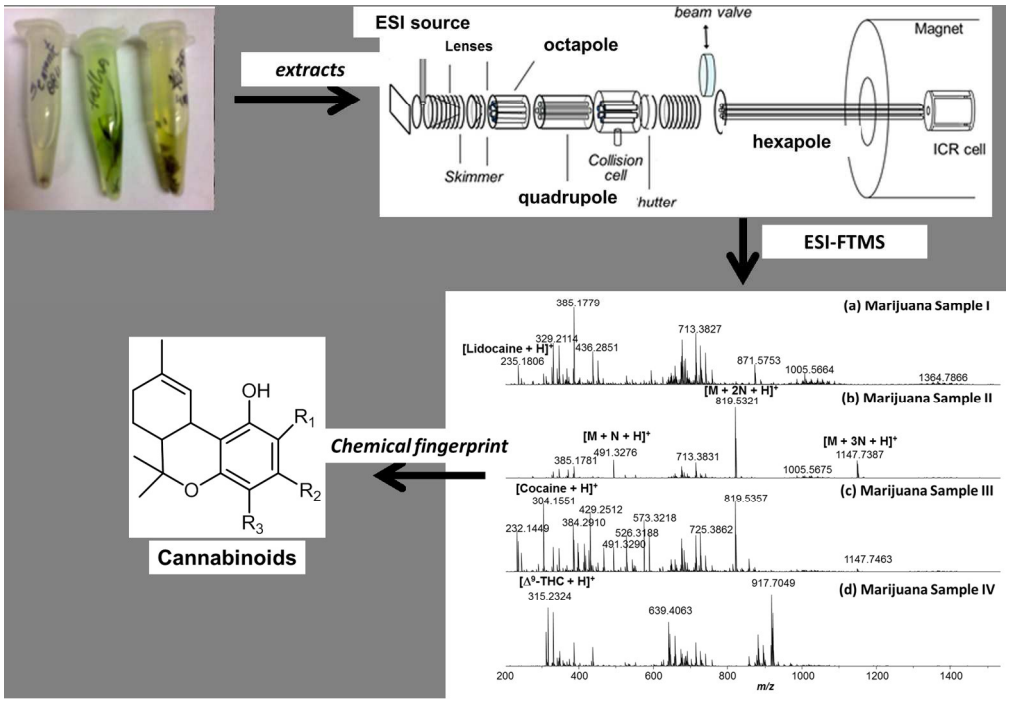

Table 1.

Formula $[M - H]^-$	$m/z_{measured}$	$m/z_{theoretical}$	Error (ppm)	DBE	Proposed Cannabinoids[1]
$[C_{17}H_{22}O_2 - H]^-$	257.1548	257.1547	-0.26	7	CBD-C_1 or Δ^9-THCO-C_1
$[C_{19}H_{22}O_2 - H]^-$	281.1548	281.1547	-0.42	9	CBN-C_3 or CBVD-C_3
$[C_{19}H_{26}O_2 - H]^-$	285.1861	285.1860	-0.47	7	CBE-C_3, CBDV-C_3 ,Δ^9-THCV–C_3 or 2-methyl-2-(4- methyl-2-pentenyl-7-propyl-2H-1-benzopyran-5-ol
$[C_{20}H_{24}O_2 - H]^-$	295.1703	295.1703	0.11	9	CBN-C_4
$[C_{18}H_{22}O_4 - H]^-$	301.1450	301.1445	-0.48	8	Δ^9-THCOA-C_1 A or B
$[C_{18}H_{24}O_4 - H]^-$	303.1607	303.1602	0.59	7	CBCN-C_3
$[C_{21}H_{24}O_2 - H]^-$	307.1707	307.1703	-0.90	10	DCBF-C_5
$[C_{21}H_{26}O_2 - H]^-$	309.1859	309.1860	0.35	9	CBN-C_5, CBF-C_5 or CBND-C_5
$[C_{20}H_{26}O_3 - H]^-$	313.1811	313.1809	-0.60	8	-
$[C_{21}H_{30}O_2 - H]^-$	313.2172	313.2173	0.40	7	Δ^9-trans-THC-C_5, CBD, Δ^8-trans-THC, *cis*–Δ^9-trans-THC-C_5, CBL-C_5 or CBC-C_5
$[C_{21}H_{28}O_3 - H]^-$	327.1966	327.1966	-0.26	8	OTHC
$[C_{21}H_{30}O_3 - H]^-$	329.2123	329.2122	-0.20	7	(E)- CBGVA-C_3, CBCON-C_5 or CBE-C_5
$[C_{20}H_{26}O_4 - H]^-$	329.1759	329.1758	-0.17	8	CBEA-C_3B, CBDVA-C_3, Δ^9-THCVA–C_3A
$[C_{20}H_{28}O_4 - H]^-$	331.1917	331.1915	-0.74	7	CBCN-C_5
$[C_{21}H_{32}O_3 - H]^-$	331.2283	331.2279	-1.40	6	-
$[C_{21}H_{28}O_4 - H]^-$	343.1917	343.1915	-0.58	8	CBCVA-C_3A or Δ^9-THCA-C_4A/B
$[C_{21}H_{30}O_4 - H]^-$	345.2070	345.2071	0.27	7	CBEA-C_5A or CBEA- C_5B
$[C_{22}H_{26}O_4 - H]^-$	353.1757	353.1758	0.31	10	$[CBNA - H]^-$
$[C_{22}H_{30}O_4 - H]^-$	357.2070	357.2071	0.35	8	$[CBDA\text{-}C_5 - H]^-$, $[\Delta^9\text{-}THCA\text{-}C_5A - H]^-$, $[\Delta^9\text{-}THCA\text{-}C_5B - H]^-$ or $[CBLA\text{-}C_5A - H]^-$
$[C_{22}H_{32}O_4 - H]^-$	359.2232	359.2228	-1.0	7	-
$[C_{21}H_{30}O_5 - H]^-$	361.2026	361.2020	-0.83	7	(-)-6a,7,10a-trihydroxy-Δ^9-tetrahydrocannabinol or (-)-Cannabitetrol
$[C_{22}H_{24}O_5 - H]^-$	367.1557	367.1551	-1.50	11	-
$[C_{22}H_{26}O_5 - H]^-$	369.1713	369.1707	-1.60	10	-
$[C_{22}H_{28}O_5 - H]^-$	371.1863	371.1864	0.21	9	Δ^9-THCA-A-8-one
$[C_{22}H_{30}O_5 - H]^-$	373.2022	373.2020	-0.30	8	11-hydroxy-Δ^9-THCA-A
$[C_{21}H_{28}O_6 - H]^-$	375.1818	375.1813	-1.30	8	-
$[C_{21}H_{30}O_6 - H]^-$	377.1975	377.1910	-1.40	7	-
$[C_{22}H_{26}O_6 - H]^-$	385.1662	385.1657	-1.40	10	-
$[C_{22}H_{28}O_6 - H]^-$	387.1812	387.1813	0.40	9	Δ^9-THCA-A-COOH
$[C_{22}H_{30}O_6 - H]^-$	389.1971	389.1970	-0.36	8	8β,11-Bis-hydroxy-Δ^9-THC-A
$[C_{24}H_{32}O_5 - H]^-$	399.2179	399.2177	-0.39	9	Δ^9-THCA +C_2H_2O
$[C_{42}H_{54}O_5 - H]^-$	637.3902	637.3899	-0.40	16	Dimer: 328 Da + 310 Da
$[C_{42}H_{58}O_5 - H]^-$	641.4216	641.4212	-0.63	14	Dimer: 314 Da + 328 Da
$[C_{42}H_{54}O_6 - H]^-$	653.3852	653.3848	-0.65	16	Dimer: 326 Da + 328 Da
$[C_{42}H_{58}O_7 - H]^-$	673.4114	673.4110	-0.70	14	Dimer: 346 Da + 328 Da
$[C_{43}H_{54}O_7 - H]^-$	681.3801	681.3797	-0.59	17	Dimer: 354 Da + 328 Da
$[C_{43}H_{58}O_7 - H]^-$	685.4114	685.4110	-0.66	15	Dimer: 358 Da + 328 Da
$[C_{43}H_{58}O_9 - H]^-$	717.4012	717.4008	-0.54	15	Dimer: 390 Da + 328 Da

[1] The chemical structure of cannabinoids identified are shown in supplementary material, **Table 1S**.

Figures

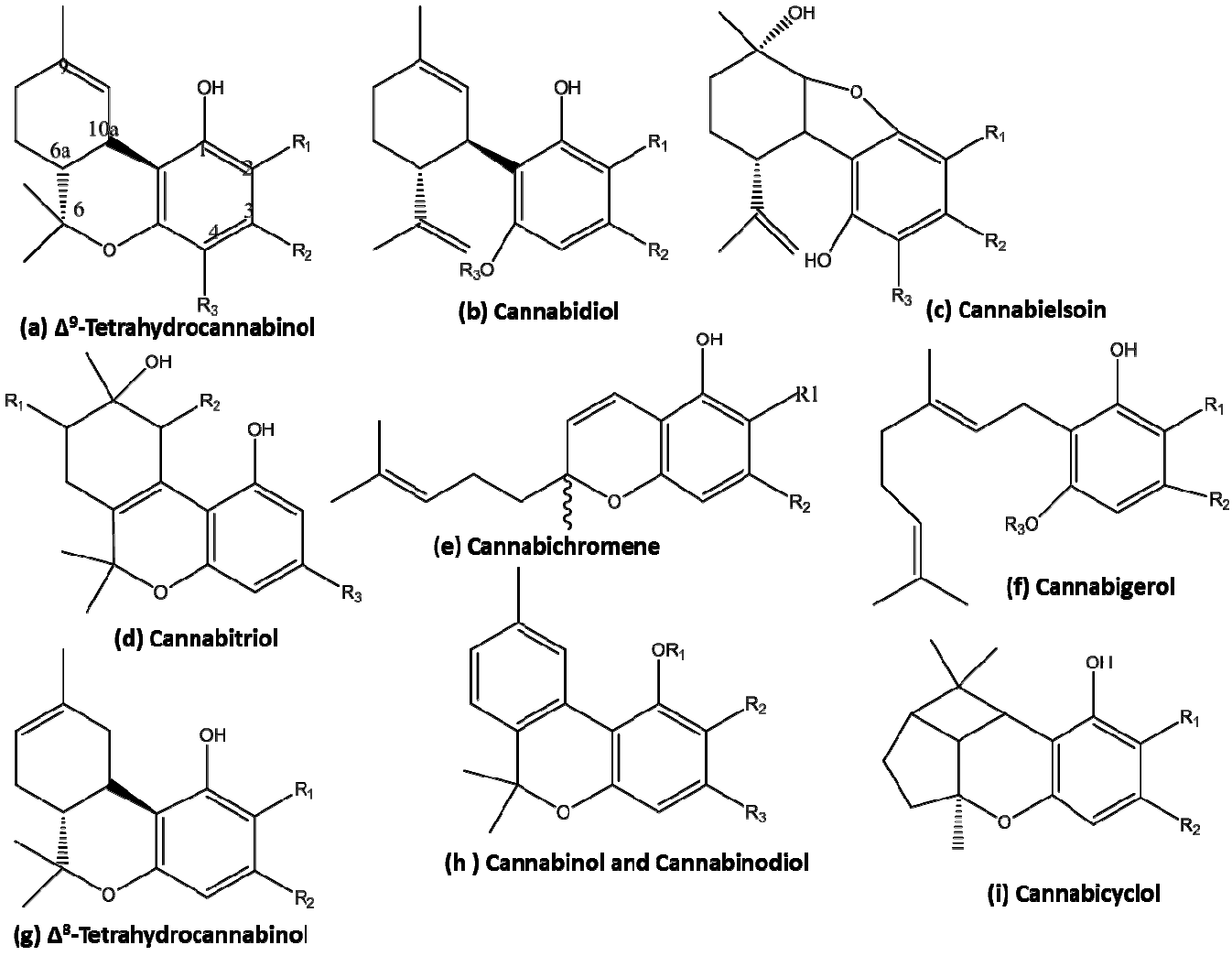

Figure 1.

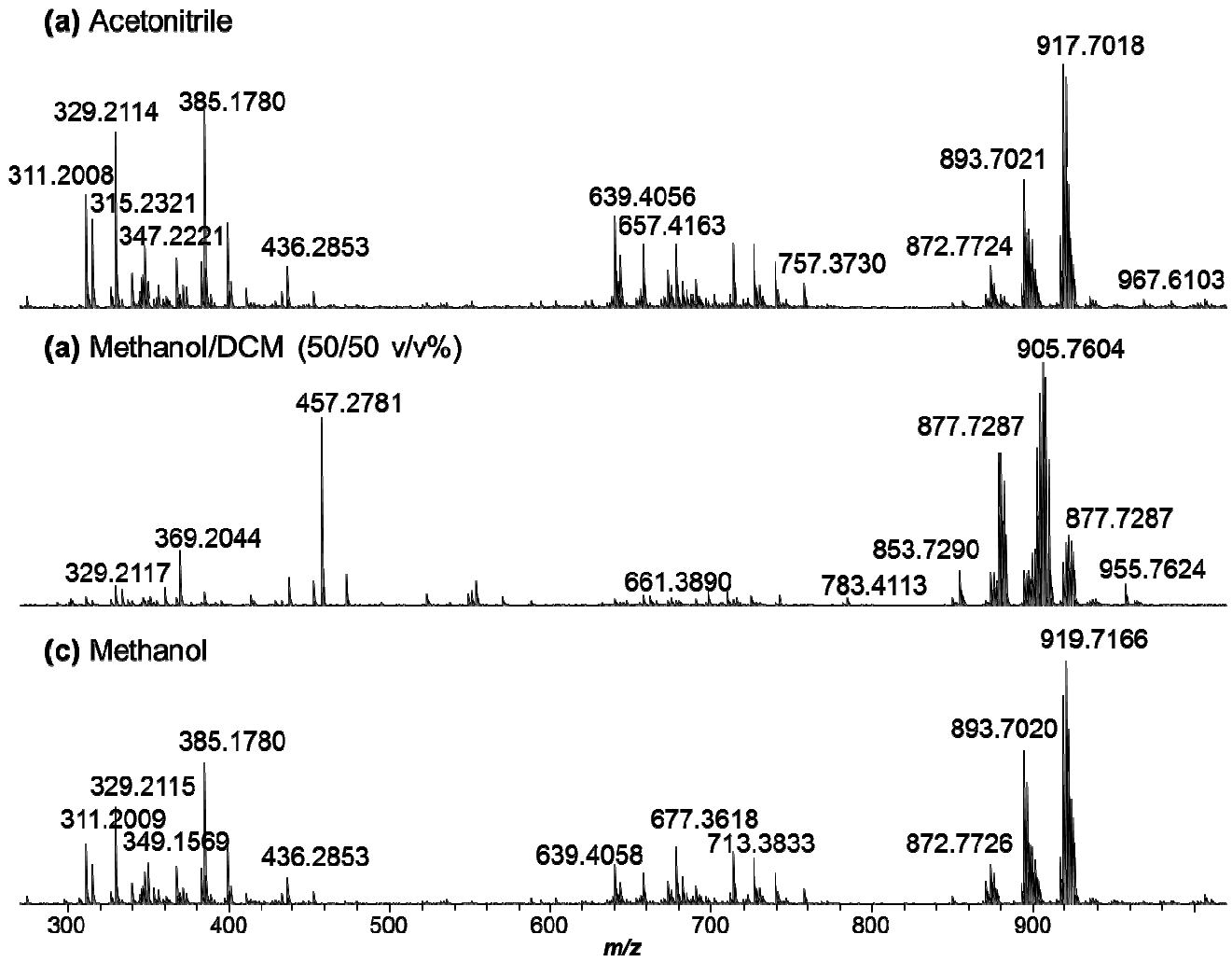

Figure 2.

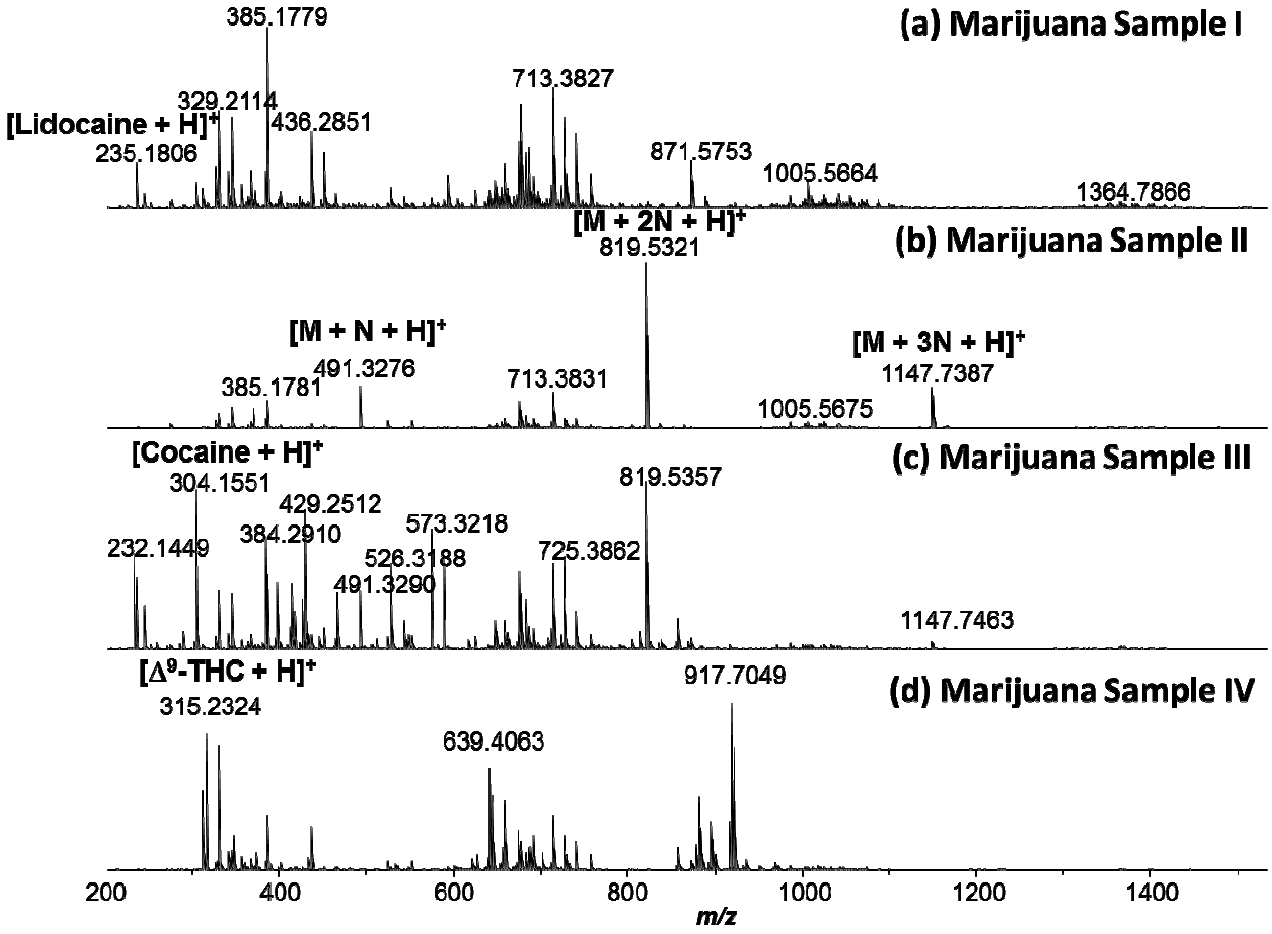

Figure 3.

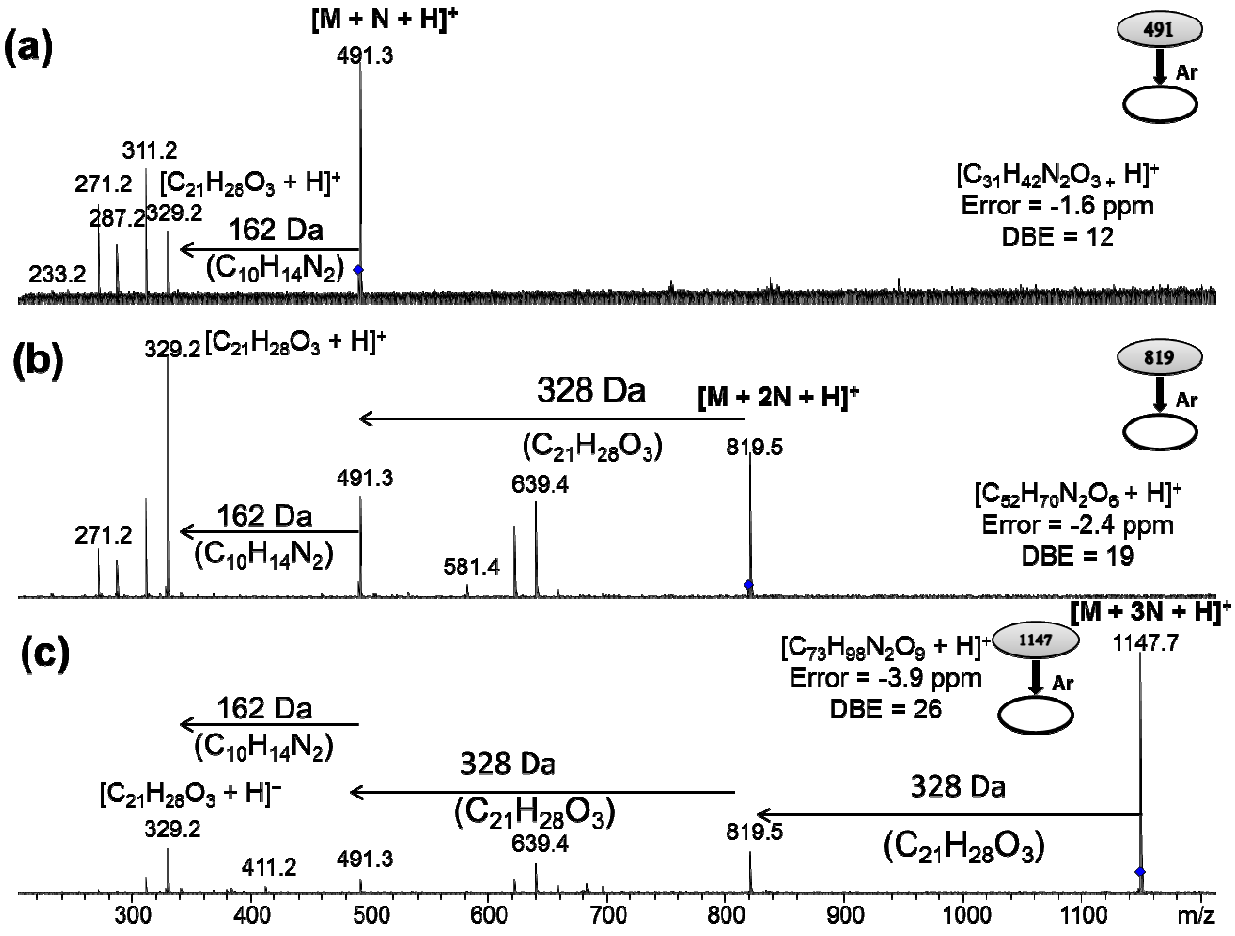

Figure 4.

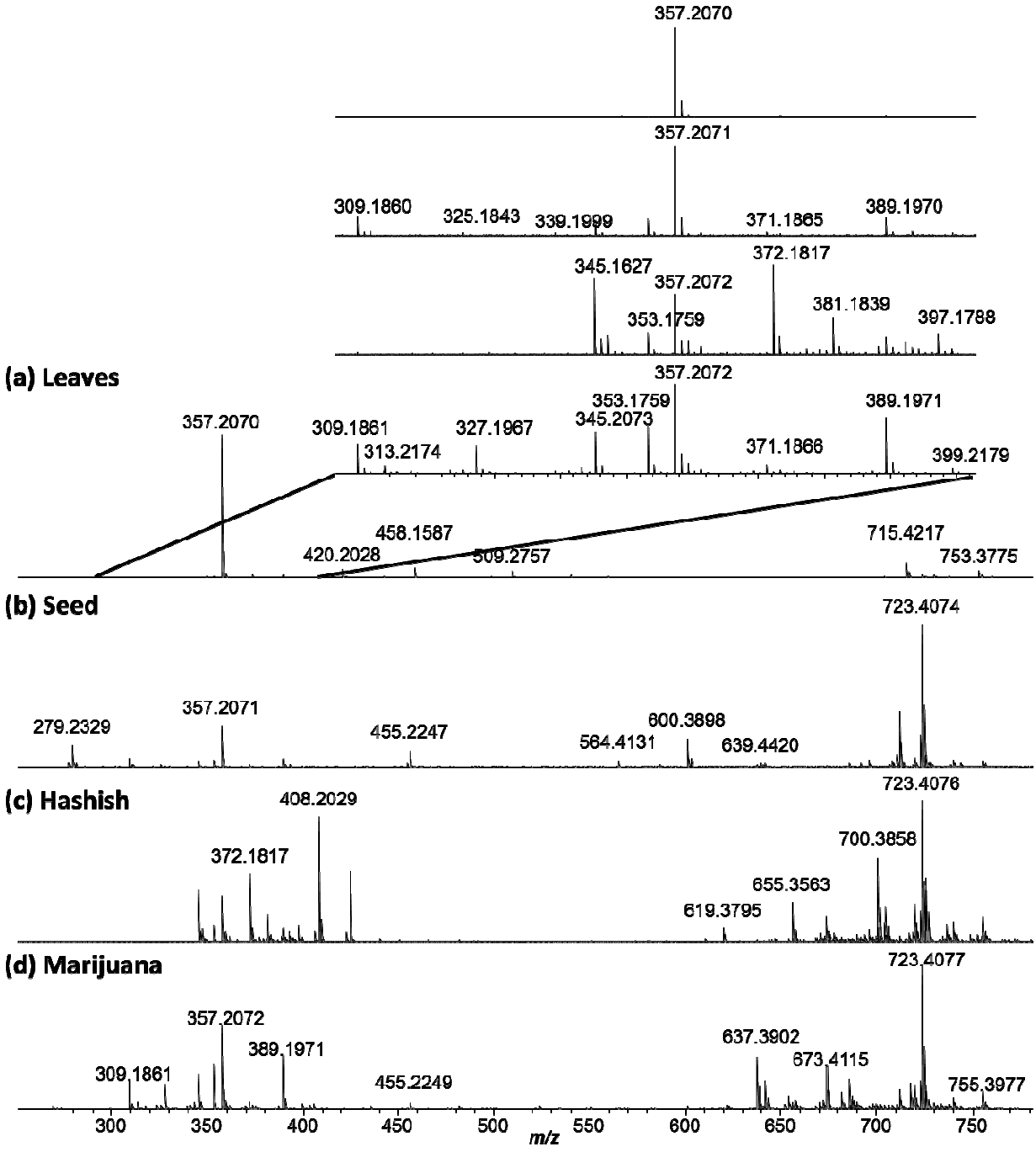

Figure 5.

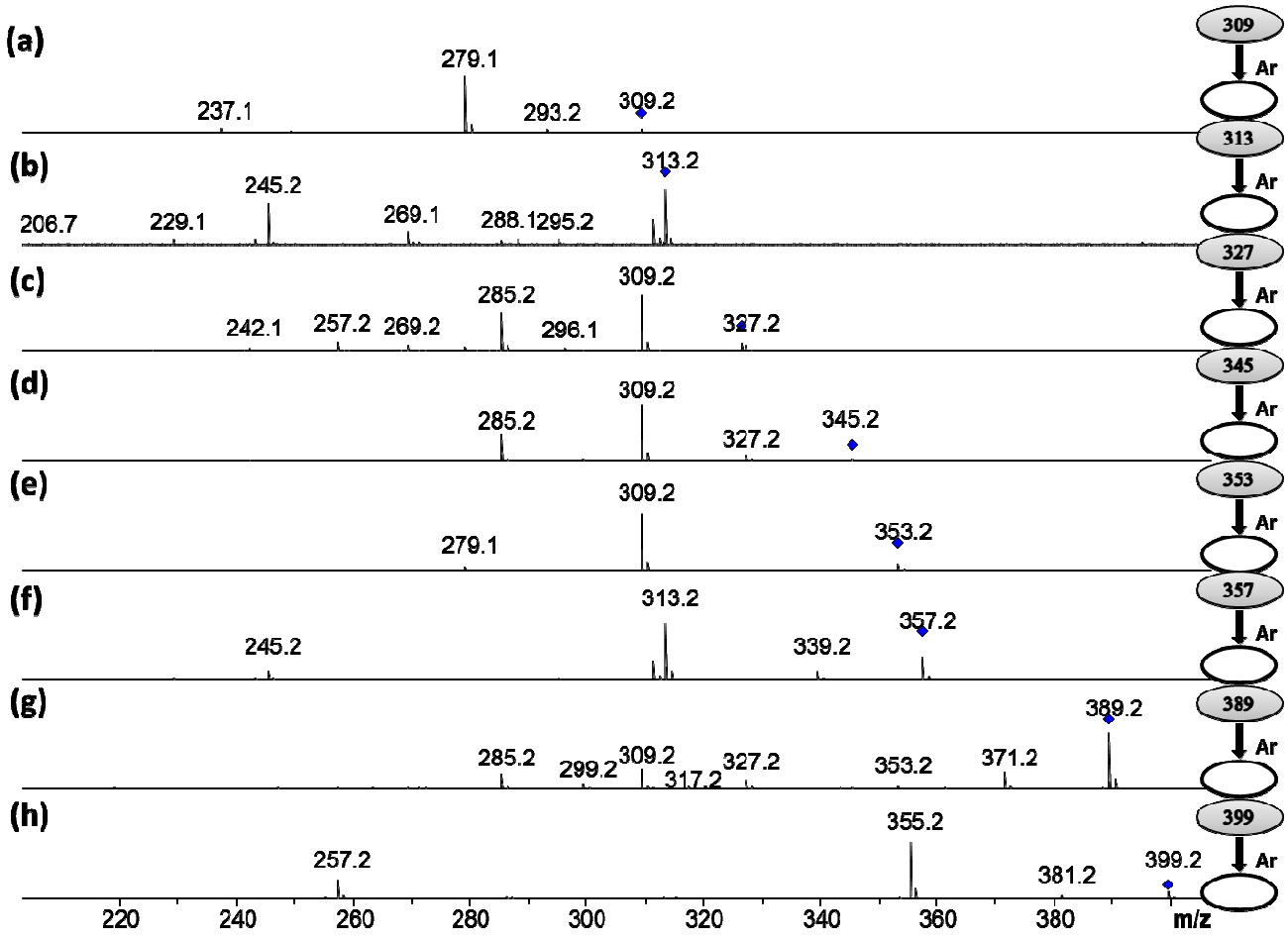

Figure 6.

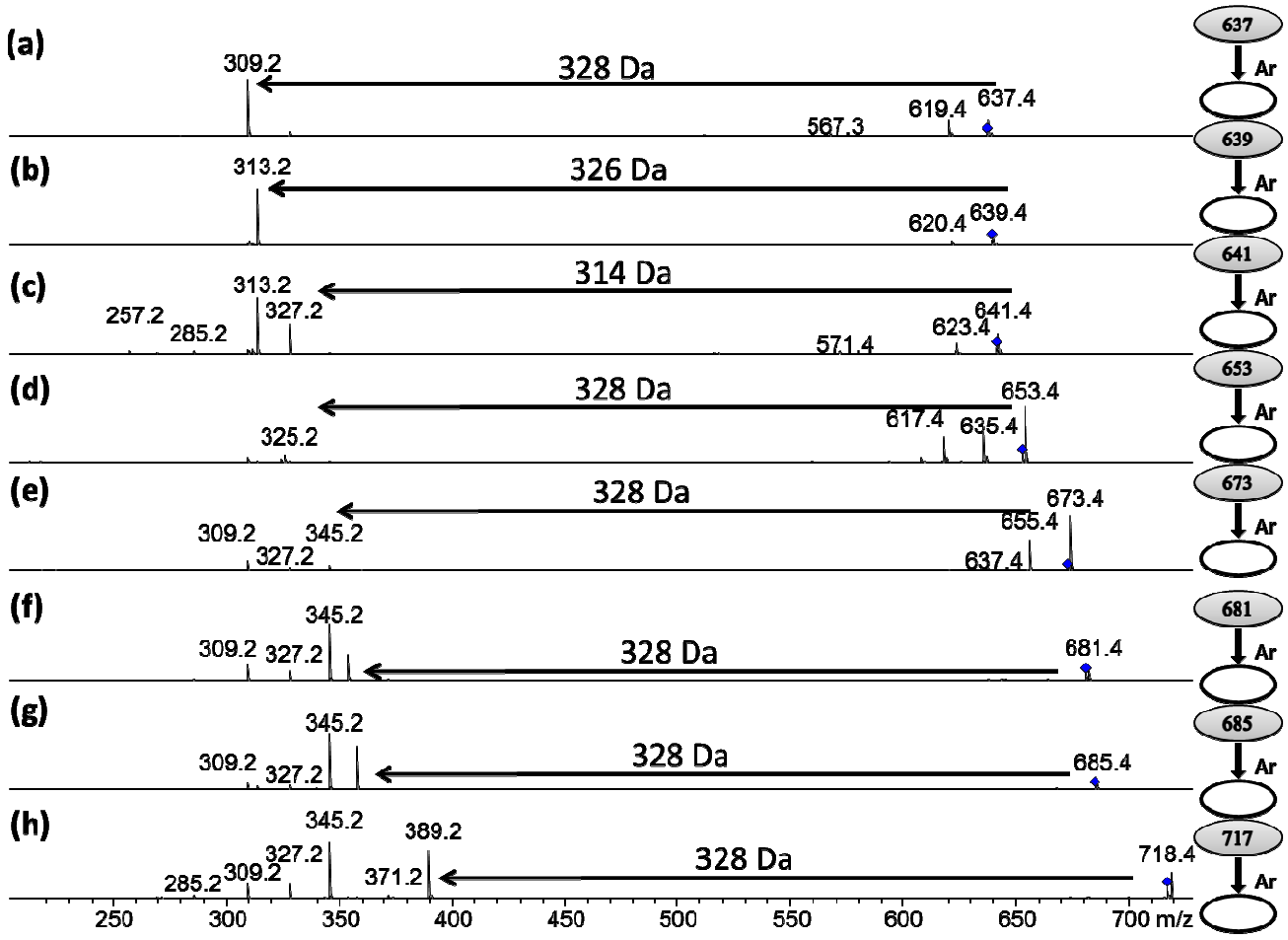

Figure 7.

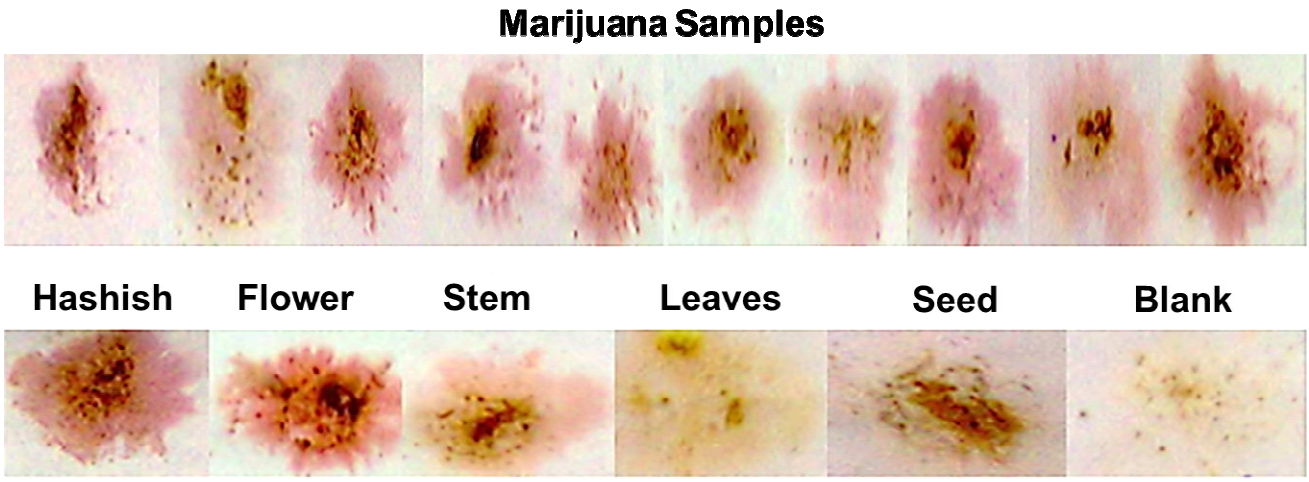

Figure 8.

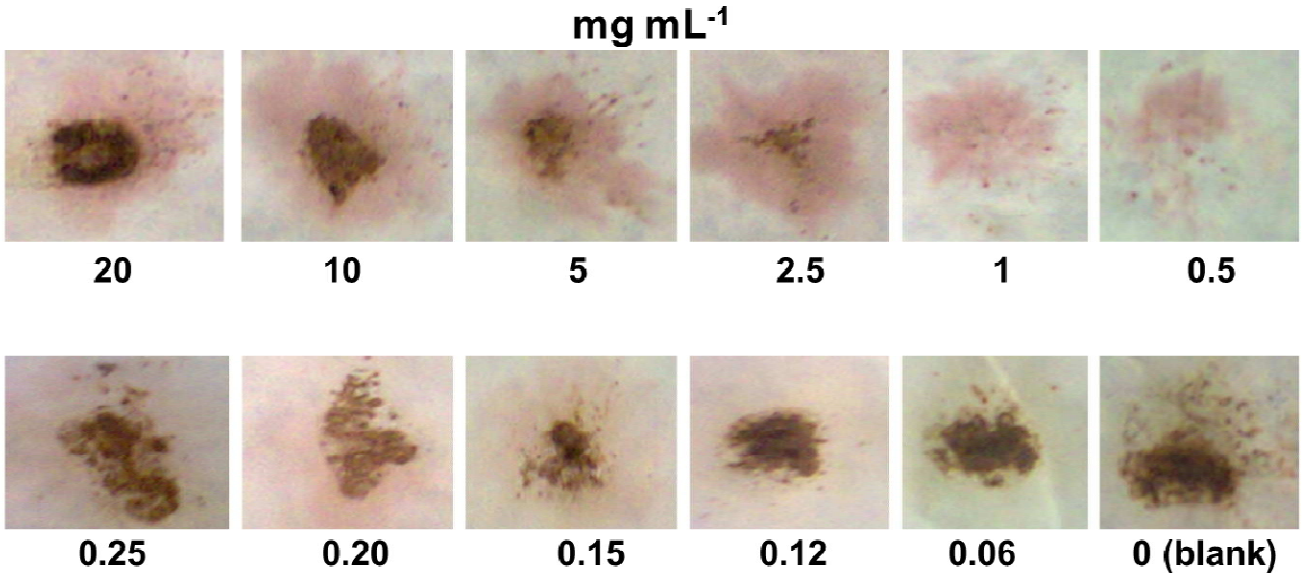

Figure 9.

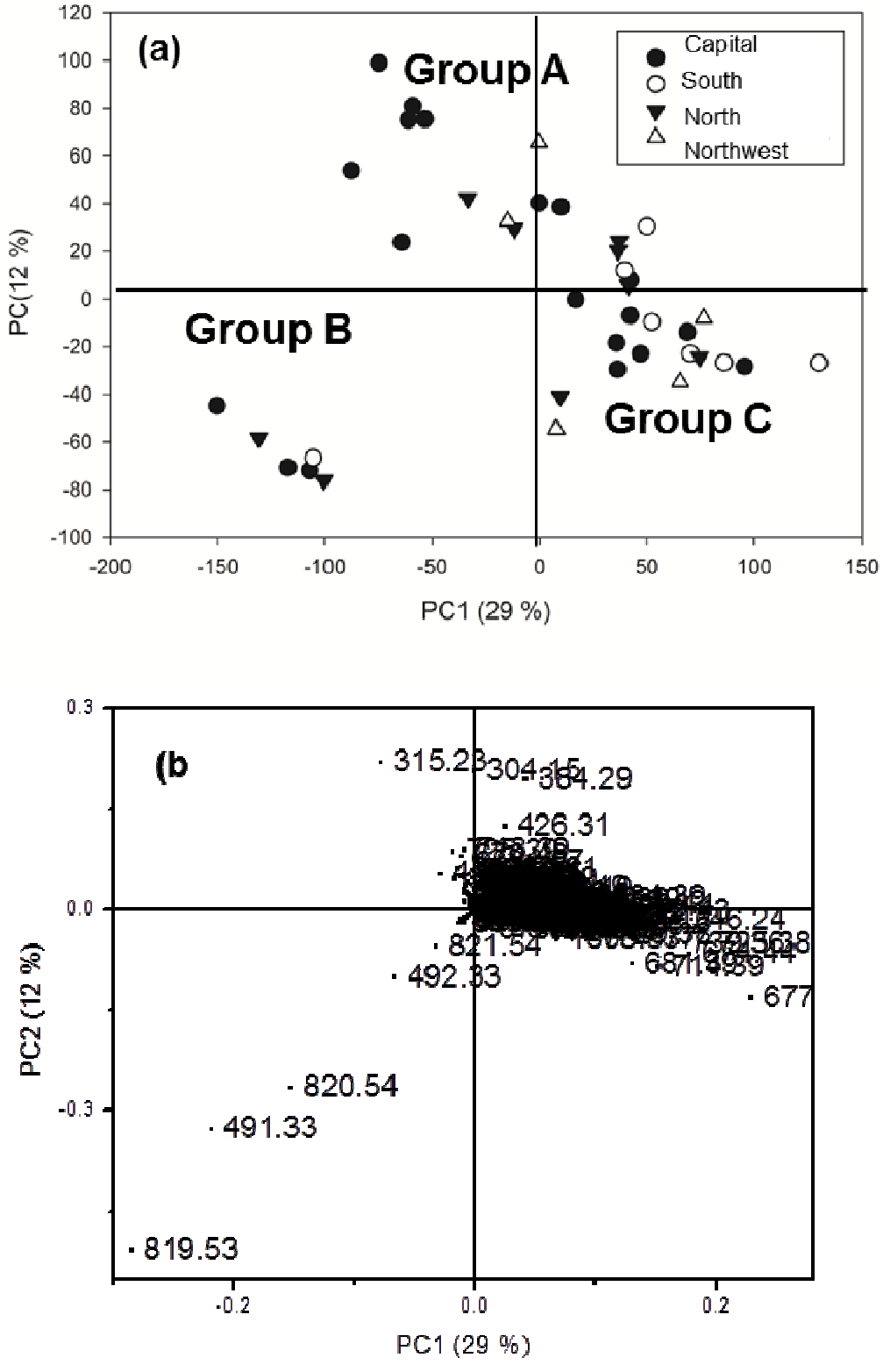

Figure 10.